PERGAMON

Geothermics 28 (1999) 253–276

GEOTHERMICS

Characterization of rock thermal conductivity by high-resolution optical scanning

Yuri A. Popov[a], Dan F.C. Pribnow[b,*], John H. Sass[c], Colin F. Williams[d], Hans Burkhardt[e]

[a]*State Geological Prospecting Academy, Miklukho–Maklai St. 39-1-191, 117485 Moscow, Russia*
[b]*Joint Geoscience Research Institute, GGA, Stilleweg 2, 30655 Hannover, Germany*
[c]*U.S. Geological Survey, 2255 N. Gemini Drive, Flagstaff, AZ 86001, USA*
[d]*U.S. Geological Survey, 345 Middlefield Rd., Menlo Park, CA 94025, USA*
[e]*Technical University, Institut für Angewandte Geophysik, Ackerstr. 71–76, 13355 Berlin, Germany*

Received 3 October 1998; accepted 7 November 1998

Abstract

We compared three laboratory methods for thermal conductivity measurements: divided-bar, line-source and optical scanning. These methods are widely used in geothermal and petrophysical studies, particularly as applied to research on cores from deep scientific boreholes. The relatively new optical scanning method has recently been perfected and applied to geophysical problems. A comparison among these methods for determining the thermal conductivity tensor for anisotropic rocks is based on a representative collection of 80 crystalline rock samples from the KTB continental deep borehole (Germany). Despite substantial thermal inhomogeneity of rock thermal conductivity (up to 40–50% variation) and high anisotropy (with ratios of principal values attaining 2 and more), the results of measurements agree very well among the different methods. The discrepancy for measurements along the foliation is negligible (<1%). The component of thermal conductivity normal to the foliation reveals somewhat larger differences (3–4%). Optical scanning allowed us to characterize the thermal inhomogeneity of rocks and to identify a three-dimensional anisotropy in thermal conductivity of some gneiss samples. The merits of optical scanning include minor random errors (1.6%), the ability to record the variation of thermal conductivity along the sample, the ability to sample deeply using a slow scanning rate, freedom from constraints for sample size and shape, and quality of mechanical treatment of the sample surface, a contactless mode of measurement, high speed of operation, and the ability to measure on a cylindrical sample surface. More traditional methods remain superior for characterizing bulk conductivity at elevated temperature.

Keywords: thermal conductivity; measurements; optical scanning; geophysics

* Corresponding author. Tel.: +49-511-643-3513; Fax: +49-511-643-3665; E-mail: dan.pribnow@bgr.de

0375-6505/99/$20
PII: S0375-6505(99)00007-3

1. Introduction

Precise and accurate thermal conductivity (λ) measurements of rocks and soils are necessary for the calculation of heat flow in both fundamental and applied geothermal studies, and for petrophysical studies of geological materials. Thermal conductivity is controlled primarily by the mineral composition and texture of the rock. Generally, λ is an anisotropic property, but for many rocks the effects of anisotropy are minor compared to the uncertainty introduced by variations in mineral composition. The bulk value of λ for earth material generally increases with water saturation and pressure and decreases with temperature.

Recently, advances in determining λ have been made through the development of a reliable *in situ* method (Burkhardt et al., 1990), thermal relaxation methods (Wilhelm, 1990), various types of logging (Williams and Anderson, 1990; Pribnow et al., 1993), and the study of mineral composition and texture of rocks (Schön, 1996). While valuable to specialized applications and important for interpolation between widely spaced samples, these approaches are no substitutes for laboratory measurements on rock samples when cores and cuttings are available.

Over the past century and more, the evolution of measurement techniques for thermal conductivity has been guided by the available technology. The availability of insulating material and the ability to maintain a constant heat input or a constant temperature difference along a cylindrical 'stack' of materials of differing thermal conductivity led to the steady-state divided-bar method, which has been described often (see e.g., Bullard, 1939; Birch, 1950; Sass et al., 1971a; Blackwell and Spafford, 1987). J.C. Jaeger was among the first to recognize the potential of transient heat-source techniques for use with solid rocks, and he suggested several configurations involving primarily line-sources (Carslaw and Jaeger, 1947; Jaeger, 1958, 1959). The availability of stable, portable electrical power supplies and strip-chart recorders, coupled with the need for fast, reliable measurements of unconsolidated sedimentary material, led to cylindrical heat-source techniques for soils and permafrost (Lachenbruch, 1957; de Vries and Peck, 1958) and to the 'needle probe' techniques for shipboard measurements on ocean sediments (von Herzen and Maxwell, 1959). The availability of portable computers allowed the evolution of 'half-space' line-source methods (see Pribnow and Sass, 1995, for a review) and pulsed line-sources (Lewis et al., 1993). All of these methods have a sound theoretical basis, but their development and validation were based primarily on systematic and meticulous experiments involving a range of standard materials.

Optical scanning is a relatively new approach to thermo-physical measurements (Popov, 1983, 1984a). A series of theoretical and experimental investigations was carried out in the 1980s and 1990s to evaluate its potential, and prototype measuring units were constructed (Popov et al., 1985a, 1993). After establishing that the precision and accuracy were satisfactory, the optical scanning method was adapted for the study of thermal conductivity and diffusivity of cores from continental deep boreholes (Popov et al., 1985a), from exploration boreholes of ore deposits and oil–gas fields in Russia (Popov et al., 1991), and mineral samples (Popov et al., 1987). The advantages of the optical scanning method include high speed of operation, contactless mode of

measurement, and the ability to measure directly on a core sample and to estimate the thermal anisotropy and inhomogeneity of rocks. It is an attractive alternative for nondestructive measurements of thermal properties of large numbers of mineral, rock and ore samples.

Both the optical scanning and line-source methods are transient, so that variations in heat capacity may affect the accuracy of thermal conductivity measurements. Thus, the comparison of optical scanning data with results of a steady-state method, e.g. the divided-bar technique, is especially helpful for the evaluation of measurement quality.

The determination of the main thermal conductivity tensor values with the divided-bar technique is possible only by means of independent measurements on variously oriented, disk-shaped plates sawed from one core sample. Rock inhomogeneity at a sample scale may affect the results, and it is important to estimate this effect. The temperature sensors (thermocouples) are inserted into copper disks that reduce the temperature gradient along the surface of disk-shaped samples and minimize the sensitivity of the sensor position relative to grains, cracks, and other local heterogeneities. The required diameter-to-thickness ratio of disks has been established only for isotropic samples. When the lateral component of conductivity significantly exceeds the vertical component, heat loss from the sample is proportionally higher than in the isotropic case, and a systematic error in measurements may arise.

The comparative study is important for the line-source technique because the effects of some experimental conditions related to this method remain controversial. These include the required size of samples, the effect of thermal contact resistance, the consistency of theoretical and experimental models in the case of measurements on anisotropic samples, and possible consequences of the transient state.

With respect to the optical scanning method, it is important to establish whether there is a significant effect imposed by a transient regime of measurements, and to evaluate its reliability and accuracy in determining the principal components of the thermal conductivity tensor. The volume of material involved in a measurement with the optical scanning method is less in comparison with the other two methods, and the effect of this difference has also to be evaluated.

Comparisons were made using the following equipment:

1 the U.S. Geological Survey divided-bar apparatus (Pribnow and Sass, 1995);
2 the line-source apparatus made at the Technical University in Berlin for the KTB field laboratory (Huenges et al., 1990), and
3 the laser unit based on the optical scanning method designed in the Moscow State Geological Prospecting Academy (Popov et al., 1985a).

2. Thermal conductivity methods under comparison

2.1. *The Divided-Bar Method (DB)*

The DB is a steady-state comparative method in which the temperature drop across a disk of saturated rock is compared with that across a disk of standard material of

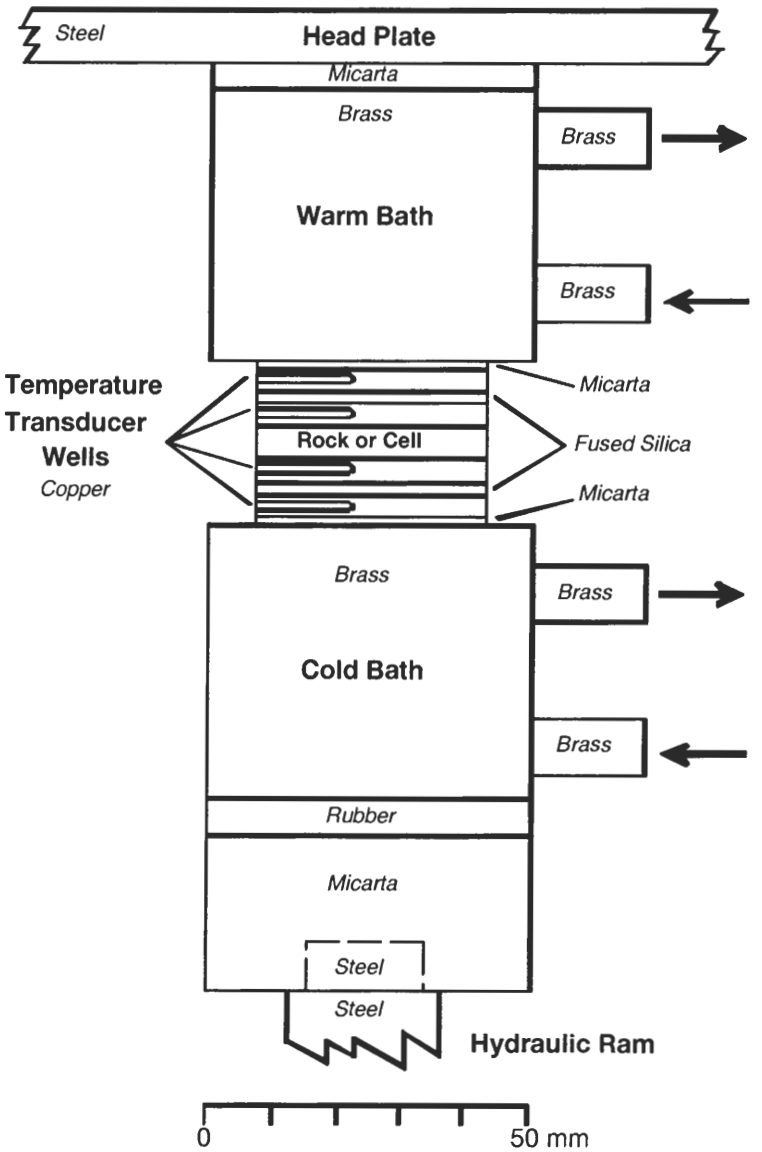

Fig. 1. The divided-bar apparatus for rock disks or cells filled with drill cuttings and water. Fused silica with well-known thermal conductivity is used as a standard.

known conductivity (Figure 1; see Pribnow and Sass, 1995, for a current, detailed description). Samples are typically 30 to 50 mm in diameter and 10 to 30 mm in thickness. The samples are saturated with water under vacuum and are held in place under an axial load of 4 to 6 MPa. This combination allows closing of microcracks

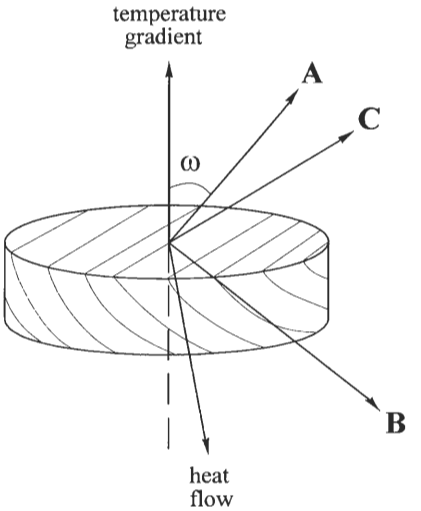

Fig. 2. Mutual orientation of vectors of temperature gradient, heat flow and principal axes of thermal conductivity for the divided-bar method. A, B and C: main (orthogonal) axes of thermal conductivity; A is perpendicular, B and C are parallel to the foliation; thin lines indicate foliation or bedding.

and filling of pore spaces and cracks with fluid, thereby eliminating errors associated with measuring dry samples at low axial pressures (Walsh and Decker, 1966). In contrast to some early versions of the instrument, in which the temperature drop across the stack was maintained by a constant heat input, most modern DBs operate on the principle of constant temperature drop and reach steady-state conditions very quickly. A measurement can be completed in 10 to 15 min. Inter-laboratory comparisons (Blackwell and Spafford, 1987), which included an early version of the USGS apparatus used in this study, established that systematic errors are quite small ($\sim 1\%$).

The vector of temperature gradient, ∇T, is directed along the disk axis at any orientation of the principal thermal conductivity axes A, B and C. Because of this, measurements on anisotropic samples prepared in such a way that the disk axis coincides with A, B, or C yield the principal values of the thermal conductivity tensor, λ_A, λ_B and λ_C, along a given axis. In a more general case, the effective thermal conductivity, λ, is determined when the disk axis and the vector of temperature gradient are inclined to a main axis of thermal conductivity (Figure 2). Here, both vectors of temperature gradient and heat flow are inclined relative to each other. The effective thermal conductivity λ connects an absolute value of the vector of temperature gradient with an absolute value of a vector of heat flow (q) across the sample:

$$|q| = \lambda \cdot |\nabla T| \tag{1}$$

Using appropriate transformations, we obtain

$$|q| = \sqrt{q_A^2 + q_B^2 + q_C^2} = \sqrt{\lambda_A^2 \cdot (\nabla T_A)^2 + \lambda_B^2 \cdot (\nabla T_B)^2 + \lambda_C^2 \cdot (\nabla T_C)^2} \tag{2}$$

where ∇T_A, ∇T_B and ∇T_C are the principal components of the temperature gradient corresponding to the main axis of thermal conductivity A, B and C, respectively. In this case, A is the axis perpendicular to the foliation, and B and C are axes parallel to the foliation.

Taking into account the relations following from Fig. 2:

$$\nabla T_A = |\nabla T| \cdot \cos(\omega)$$

$$\nabla T_B = |\nabla T| \cdot \cos(\phi)$$

$$\nabla T_C = |\nabla T| \cdot \cos(\psi) \tag{3}$$

we obtain from eq. (2):

$$|q| = \sqrt{\lambda_A^2 \cdot \cos^2(\omega) + \lambda_B^2 \cdot \cos^2(\phi) + \lambda_C^2 \cdot \cos^2(\psi)} \cdot |\nabla T| \tag{4}$$

where ω, ϕ and ψ are angles between the vertical disk (sample) axis and the principal axes of conductivity A, B and C, respectively.

According to eq. (1), we gain from eq. (4) the effective thermal conductivity measured with the divided bar apparatus:

$$\lambda = \sqrt{\lambda_A^2 \cdot \cos^2(\omega) + \lambda_B^2 \cdot \cos^2(\phi) + \lambda_C^2 \cdot \cos^2(\psi)} \tag{5}$$

A two-dimensional anisotropy model is adapted here for the samples: $\lambda_A = \lambda_{PER}$ and $\lambda_B = \lambda_C = \lambda_{PAR}$, where λ_{PER} and λ_{PAR} represent the thermal conductivity components perpendicular and parallel to a bedding or, in the case considered in this paper, to the foliation. Using the known relation

$$\cos^2(\omega) + \cos^2(\phi) + \cos^2(\psi) = 1 \tag{6}$$

it can be readily shown, according to eq. (5), that in the case of two-dimensional anisotropy we measure an effective thermal conductivity referred to principal values of the conductivity tensor:

$$\lambda = \sqrt{\lambda_{PER}^2 \cdot \cos^2(\omega) + \lambda_{PAR}^2 \cdot \sin^2(\omega)} \tag{7}$$

where ω is the angle between the vertical disk axis and the principal axis of thermal conductivity corresponding to λ_{PER}.

2.2. *The Line-Source Method (LS)*

This method is based on the theory of a line-source in an infinite medium (Carslaw and Jaeger, 1947). The apparatus used here is a half-space LS, i.e. a needle probe embedded in and flush with the surface of a material of very low thermal conductivity (Plexiglass). Details of the construction and a special evaluation algorithm are described in Huenges et al. (1990). It can be shown that the requirement of an infinite probe length is realized in a satisfying way if the length-to-diameter ratio of the needle probe is larger than 30:1 and if the probe temperature is recorded at the center of the probe. Possible consequences of such point temperature measurements are discussed in a later section on the random error of LS.

According to Grubbe et al. (1983), the result obtained from measurement of an anisotropic sample is related to the principal values of the thermal conductivity tensor:

$$\lambda = \sqrt{\lambda_A \cdot \lambda_B \cos^2(\gamma) + \lambda_A \cdot \lambda_C \cdot \cos^2(\beta) + \lambda_B \cdot \lambda_C \cdot \cos^2(\alpha)} \quad (8)$$

where α, β and γ are angles between the line-source axis and principal axes of thermal conductivity A, B, and C, respectively. As follows from this relationship, in a general case the principal thermal conductivity tensor values can be determined by means of three measurements with non-collinear and non-coplanar positions of the LS, providing a knowledge of α, β and γ. It is evident that the most precise measurements are provided by a consecutive arrangement of the LS along each principal axis of thermal conductivity.

For the two-dimensional anisotropy model ($\lambda_A = \lambda_{PER}$; $\lambda_B = \lambda_C = \lambda_{PAR}$) and to rule out an uncertainty in estimating the principal axes from visual inspection of the cores, the LS was placed on the top plane of the core (perpendicular to the core axis) and λ was measured with varying azimuth (Figure 3; see also Pribnow and Sass, 1995). Considering that the thermal conductivity parallel to the foliation is higher than that perpendicular to it and that the measured thermal conductivity for an LS represents a value from a plane approximately perpendicular to the line-source axis, the strike of the foliation was defined by the LS position with the lowest thermal conductivity value. The core was then cut parallel to its axis and perpendicular to the estimated strike of foliation (Fig. 3). Again, λ was measured for varying angles. The maximum measured λ represents λ_{PAR}. For the position perpendicular to the latter, the measured λ is defined as λ_{MIN}. According to eq. (8), λ_{PER} can be determined from eq. (9) if λ_{PAR} is known ($\alpha = \beta = 90°$; $\gamma = 0°$):

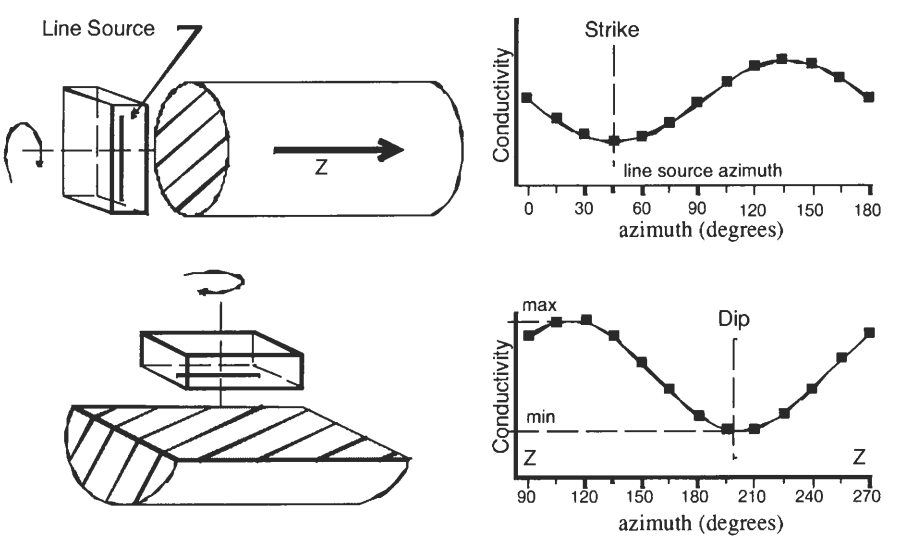

Fig. 3. Determination of main thermal conductivity components with the half-space line-source.

$$\lambda_{MIN} = \sqrt{\lambda_{PER} \cdot \lambda_{PAR}} \tag{9}$$

2.3. The Optical Scanning Method (OS)

The Optical Scanning Method (OS) is relatively new to both Earth science and the field of thermal physics. The theoretical model is based on scanning a sample surface with a focused, mobile and continuously operated constant heat source in combination with a temperature sensor. The heat source and sensor move with the same speed relative to the sample and at a constant distance to each other (Figure 4; Popov, 1983). The temperature sensor displays the value of the maximum temperature rise along the heating line behind the source. The maximum temperature rise, Θ, is determined by the relationship

$$\Theta = \frac{Q}{2\pi \cdot x \cdot \lambda} \tag{10}$$

where Q is the source power and x is the distance between source and sensor.

If the sample(s) under study and a reference standard with known conductivity, λ_R, are aligned along the scanning direction, the thermal conductivity of each sample can be determined from λ_R and the ratio of Θ to Θ_R or, in actual application, from the ratio of electric signals U and U_R, which are proportional to Θ and Θ_R. This relation is expressed as

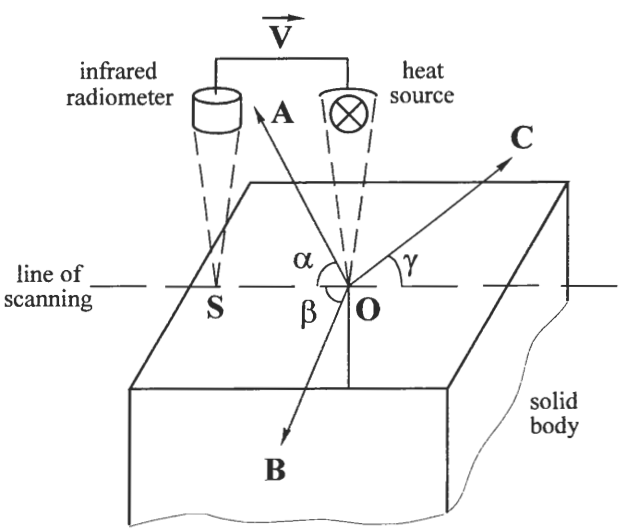

Fig. 4. Principle of optical scanning method. V: velocity of scanning; O: area of the heat spot; S: detection area of the radiometer; A, B and C: main axes of thermal conductivity with angles α, β and γ to line of scanning, respectively.

$$\lambda = \lambda_R \cdot \left(\frac{\Theta_R}{\Theta}\right) = \lambda_R \cdot \left(\frac{U_R}{U}\right) \tag{11}$$

For an anisotropic solid, the maximum temperature rise is determined by the relationship (Popov and Mandel, 1998)

$$\Theta = \frac{Q}{2\pi \cdot x \cdot \sqrt{\lambda_A \cdot \lambda_B \cdot \cos^2(\gamma') + \lambda_A \cdot \lambda_C \cdot \cos^2(\beta') + \lambda_B \cdot \lambda_C \cdot \cos^2(\alpha')}} \tag{12}$$

where α', β' and γ' are angles between the A, B and C principal axes of thermal conductivity and the scanning line. Consequently, the relationship for the thermal conductivity from a single measurement is similar to that for the LS ($\alpha = \alpha'$, $\beta = \beta'$, $\gamma = \gamma'$) and can also be expressed using eq. (8).

After scanning along three non-collinear and non-coplanar directions which are located on two non-parallel planes, eq. (8) provides a means of determining the principal values of thermal conductivity from a set of three equations with three unknowns. For a sample with two-dimensional anisotropy, the principal values of conductivity can be determined from two non-collinear scans on one face, if this face is not parallel to the foliation (Popov et al., 1985b).

The OS apparatus is shown schematically in Fig. 5 (Popov, 1983; Popov et al., 1983, 1985a). It provides simultaneous measurement of thermal diffusivity as well as conductivity, but the theory and application of the thermal diffusivity measurements are beyond the scope of this paper (see Popov, 1984a, for details). The stationary laser heat source and an infrared radiometer for measurements of initial and maximum sample temperature are placed on a mobile platform that moves at a constant speed (1 to 10 mm s^{-1}) relative to samples and reference standards. The speed chosen is based on the layer thickness required for the study. Measurements are carried out on either plane or cylindrical surfaces of the dry or saturated samples. In the case of cylindrical samples, scans are oriented along the core axis and the bottom face of the core. Surface roughness of up to 1.0 mm is allowable. In general, it is not necessary to polish a sample surface. If the scanned surface is too rough systematic errors can be corrected based on results from reference standards with a similarly rough surface. The working surface of the sample is covered with an optical coating (25–40 μm thick) in order to minimize the influence of varying optical reflection coefficients. Sample sizes in this study varied from 3–17 cm in length, 3–9 cm in width, and 2–6 cm in thickness.

The specific feature of OS is the ability to change the thickness of the investigated surface-layer depending on the sample size and research goals. This can be done by a change in measurement regime including the speed of scanning and the distance between the heated spot and the area of temperature recording. The layer thickness also depends on the thermal properties of the sample and may reach 2–3 cm or more for samples with thermal conductivity exceeding 6–7 $Wm^{-1}K^{-1}$ (see Popov et al., 1993, for more details).

The signal-processing algorithm yields the effective conductivity of two perpendicular directions for an inhomogeneous layered sample. The mean level of tem-

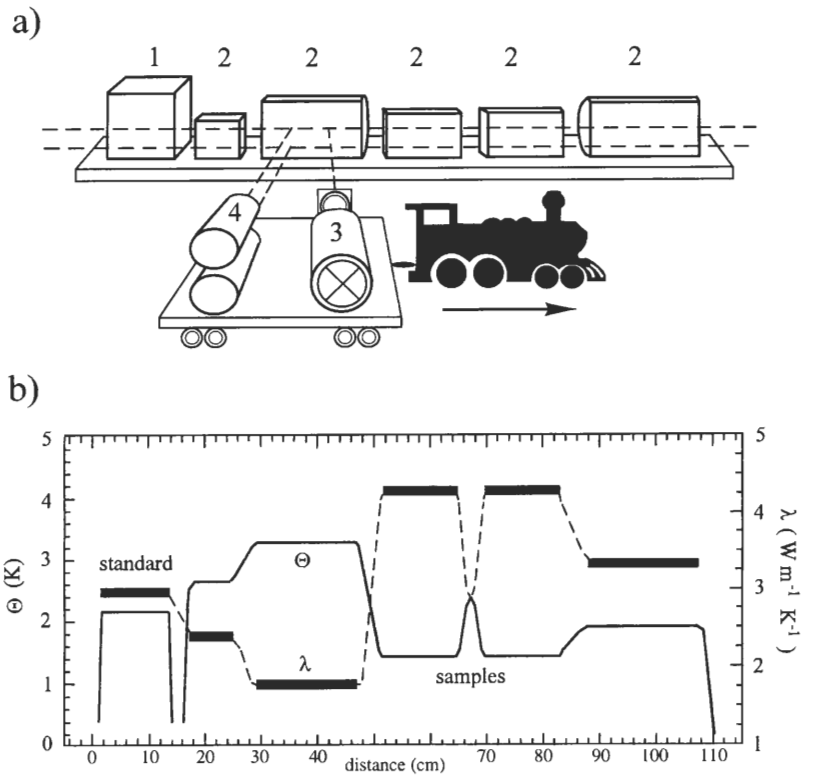

Fig. 5. (a) Scheme of the optical scanning apparatus; 1—standard with known thermal conductivity; 2—samples; 3—heat source; 4—infrared radiometers (the lower one is for the determination of thermal diffusivity). (b) Example of a measurement; Θ—temperature detected with 4 (solid line); λ—thermal conductivity (dashed lines and bars) calculated with eq. (11).

perature along the scanning profile is used in eq. (11) for the determination of thermal conductivity in the orientation coincident with the scanning direction, and the thermal conductivity normal to the heated surface is determined as an arithmetic mean of local conductivities along the entire scanning line (Popov, 1983). Experimental studies of inhomogeneous samples consisting of up to 20 layers with thermal conductivities ranging from 1.35 to 21.0 $Wm^{-1}K^{-1}$ and thicknesses varying from 1 to 15 mm have shown that this determination of effective thermal conductivity does not differ significantly from the calculated conductivity of layered samples (Popov et al., 1993). Local conductivities can be determined for grain scales as small as 7 to 10 mm.

After the scanning is completed, the following information is available for each sample:

1 a conductivity profile (including minimum and maximum values λ_{min} and λ_{max}, respectively) along a single scanning line,
2 the effective thermal conductivity of each sample for two mutually perpendicular directions and the related macro-anisotropy factor,

3 the thermal inhomogeneity factor ε (defined as the maximum difference in conductivity along the scanning line divided by the effective thermal conductivity), and
4 the RMS deviation of local thermal conductivity values along each scanning line.

At present, the measurable range of conductivity is 0.2 to 70 $Wm^{-1}K^{-1}$. The basic measurement error, including random and systematic components estimated from tests on standards, is not more than 3% at 0.95 confidence level. The rate of measurements is between 50 and 70 measurements per hour, and permissible sample lengths range from 1 to 70 cm. Discrepancies between theoretical and experimental models of the method have been discussed in detail by Popov (1983, 1984b) and Popov et al. (1993).

Quartz monocrystals were used to check the adequacy of experimental and theoretical models for anisotropic samples. Errors were less than 0.5%. Our results for the A and B axes ($6.05 \pm 0.05\ Wm^{-1}K^{-1}$) and the C axis ($10.7 \pm 0.1\ Wm^{-1}K^{-1}$) at room temperature (Popov et al., 1990) are consistent with the A and B axes ($6.07 \pm 0.1\ Wm^{-1}K^{-1}$) and C axis ($10.5 \pm 0.1\ Wm^{-1}K^{-1}$) values obtained by Beck (1987). The apparent thermal conductivity of a quartz monocrystal as measured by the OS unit at a progressing series of angles relative to the C axis is shown in Fig. 6 in comparison with theoretical values determined from eq. (8). According to these results, the random error of a single measurement (95% confidence interval) lies within the range of 0.5 to 2.0%.

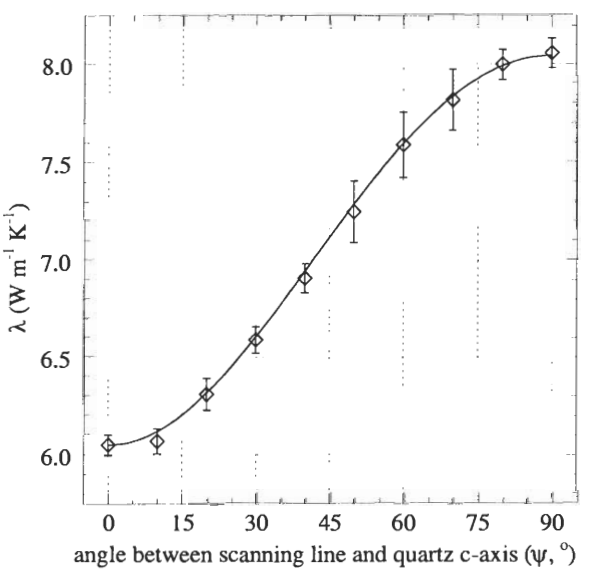

Fig. 6. Theoretical and experimental results for the effective thermal conductivity of a quartz monocrystal for different angles between the C-axis and the line of OS scanning. Continuous curve—result of the theoretical calculations according to eq. (8). Diamonds with vertical bars—the average values of thermal conductivity (6–24 measurements) with 0.95% confidential probability.

3. Sample collections and measurement procedure

Thermal conductivity measurements with the three methods (OS, LS, and DB) were performed on two sample collections, both consisting of gneiss and amphibolite from the KTB borehole (see also Pribnow and Sass, 1995).

Collection I includes 44 core samples of amphibolite, gneiss, and, to a lesser degree, other lithologies from the KTB section. Two principal values were determined by LS measurements for 34 water-saturated samples; in 10 cases, sample preparation partly destroyed the core piece. Proceeding from the two-dimensional anisotropy model, two disks—along and across the foliation—were sawed from each core sample for the DB after LS measurements. Both components of thermal conductivity, λ_{PAR} and λ_{PER}, were determined for 38 core samples from this collection; for one sample, only λ_{PER} was determined and for 5 samples, only λ_{PAR}. The lack of one of the components for these six samples resulted from problems in preparing satisfactory disk samples.

The study of samples from Collection I with OS was also based on the two-dimensional anisotropy model, with λ_{PAR} and λ_{PER} determined on end-pieces of core left over after the disks had been sawed for the DB. As previously mentioned, one sample face is enough for the measurement of λ_{PAR} and λ_{PER} with OS under the condition that this face is not parallel to the foliation. In our case, the angles between this face and the foliation were in the range of 45° to 90°. Scanning along 2–4 equally spaced lines parallel to the intersection of foliation with the working face was performed first. Then, scanning was carried out along 2–4 lines perpendicular to the first set [Fig. 7(a)]. Several lines for each direction must be scanned in order to take appropriate account of possible sample inhomogeneity. The number of scanning lines was chosen depending on the face length. To estimate and decrease random error, the measurements along each line were repeated 2–4 times. This is important for the calculation of principal conductivity values because, according to eq. (8), the total random error for λ_{PER} increases not less than by $\sqrt{5}$ times (for one measurement). The mean apparent conductivity for each of two chosen directions was derived from measurements along all parallel lines. Mean values of apparent conductivity for each of the two directions and a measured angle between the scanning lines and foliation were substituted into eq. (8). By solving this system of equations, λ_{PER} and λ_{PAR} were determined for every sample. If possible, the face with the maximum angle to the foliation was chosen, because then the error in determining the actual foliation plane least affects the results for the principal thermal conductivity components. For virtually all anisotropic samples, the thermal inhomogeneity factor was higher when the scanning line was oriented perpendicular to the intersection of foliation and working face. In this orientation, the scanning line traverses all layers of variable mineral composition whereas scanning parallel to the foliation involves a single, homogeneous layer.

Collection II is a subset of Collection I and included 36 disks prepared for measurements with the DB and OS on identical samples. The disk diameter was 36 mm and the thickness varied from 8 to 12 mm. For one set of disks, the foliation was parallel or nearly parallel (with an inclination $<10°$) to the disk plane. For another set of disks, the foliation was perpendicular or nearly perpendicular ($>80°$) to the disk plane; for one disk, the inclination angle was 60°.

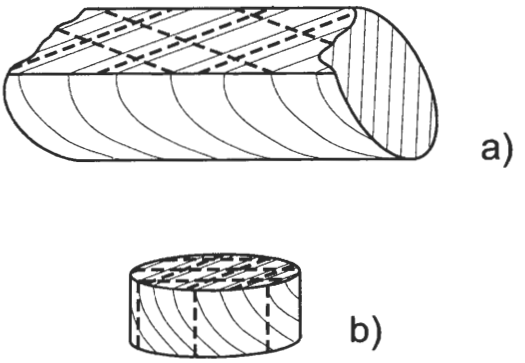

Fig. 7. Lines of scanning on samples of collections I (a) and II (b). Dashed lines show lines of scanning for measurements with the optical scanning method; thin lines show foliation planes.

The thermal conductivity of 33 of these disks was measured with the DB in a water-saturated state. Subsequent measurements on each disk with the OS included at least three scans along three lines parallel to the intersection between the foliation and the disk plane. Spacing between the lines was 7–8 mm [Fig. 7(b)] and the measurements were performed on both disk planes. Then the operation was repeated for three perpendicular lines on each disk plane. In addition, several scans along 5–8 lines were made on the cylindrical surface of every disk [Fig. 7(b)]. This required a specific choice of the distance between temperature sensor and sample ['x' in eq. (10)] for the OS apparatus because of the small disk thickness. Without these scans on the cylindrical surface it would have been impossible to determine principal thermal conductivity values in the case when the foliation was oriented subparallel to the disk plane. The third scanning direction allowed us to study a possible 3-D anisotropy of the rocks.

As in Collection I, λ_{PAR} and λ_{PER} were determined and, in the case of obvious 3-D anisotropy, expressed as significantly distinct λ_A, λ_B and λ_C. In many cases, the DB measurements did not yield principal λ_{PAR} and λ_{PER} values but some effective values according to eq. (5) or eq. (7) in the case of 3-D or 2-D anisotropy, respectively. The correct comparison of DB and OS results required computation of the effective disk conductivity corresponding to a value measured with DB and taking into account the angle of foliation. For Collection II, therefore, we took into account the real inclination angles between the foliation and disc planes in order to transform OS results of λ_{PER} and λ_{PAR} to thermal conductivity values λ_V that are effective for DB measurements. For this study, inclination angles are close to 0° or 90° and the corresponding effective thermal conductivity values are λ' and λ'', respectively. For collection I, we had neglected some uncertainty in these angles, considering them to be exactly 0° and 90° for λ_{PAR} and λ_{PER}, respectively.

Optical scans for Collections I and II were performed in surface-layers that are 6–9 and 5–7 mm thick, respectively. A short length of scanning line on the cylindrical surfaces of disks (8–12 mm) required a reduction of the distance between the heated spot and the area of temperature recording. This led to a decrease of the layer thickness to 4–5 mm.

The random error for DB is between 1 and 2% and for this version of LS is below 5%. Using a high scanning speed for the OS, more than 3000 measurements were performed for Collections I and II. Discrepancies between average and single results for each typical scanning line yielded a random error for single OS measurements of 1.6% (at 0.95 confidence level). Repeated scans were necessary mainly for the estimation of random error; the determination of principal thermal conductivity values requires only a single scan of each line.

4. Results and discussion

Table 1 lists the results of DB, LS and OS for Collection I, and Table 2 for Collection II. In addition, all results have been analyzed separately for each component, λ_{PAR} and λ_{PER}, considering:

1 number of values: N;
2 range of values: λ_{min} to λ_{max} along one scanning line;
3 anisotropy: $K=\frac{\lambda_{PAR}}{\lambda_{PER}}$;
4 inhomogeneity (for OS only): $\varepsilon=\frac{\lambda_{max}-\lambda_{min}}{\lambda_{average}}$;
5 linear regression for DB vs. OS, LS vs. OS, and LS vs. DB;
6 relative differences for DB vs. OS, LS vs. OS, and LS vs. DB: $2\cdot\frac{\lambda_i-\lambda_j}{\lambda_i+\lambda_j}$.

The results of steps (1) through (6) are summarized and discussed below.

4.1. Collection I

Correlations between λ_{PAR} and λ_{PER}, measured with different methods, are exhibited in Fig. 8. DB and OS results reveal the closest correlation. The results obtained with these methods are characterized by higher correlation coefficients (0.87 to 0.91) and substantially lower standard deviations (0.23 to 0.25) relative to comparisons with the LS (0.78 to 0.86, 0.30 to 0.37, respectively). However, while the linear coefficient for the comparison of DB and OS is close to 1 (0.93 and 0.90, respectively), the coefficient for λ_{PER} alone is somewhat worse (1.16). Nevertheless, a rather small intercept value indicates that λ_{PER} measurements with DB and OS are well correlated, too. Considering the inhomogeneity and anisotropy of the samples studied, this range is acceptable. Comparing both components from OS and LS, the correlation coefficient is 0.86 and the intercept is relatively small (0.15). However, LS and OS results for λ_{PER} have the lowest correlation coefficient (0.69).

For all methods compared, the average relative differences between results for λ_{PAR} are negligible (0.03 to 0.8%) and those for λ_{PER} acceptable (1.4 to 3.2%). The discrepancies for the anisotropy factor are in the same range (0.4 to 3.8%) but OS and LS, on average, show higher values than the DB. It should be noted that when all data are highly representative and random errors for OS and DB are small, the systematic divergence for λ_{PER} (and thus the related deviation for the anisotropy

Table 1
Results of thermal conductivity (λ) measurements from divided-bar (DB), optical scanning (OS) and line-source (LS) methods parallel (λ_{PAR}) and perpendicular (λ_{PER}) to the foliation for Collection I (see text). z—depth; lithology: AM—amphibolite; GN—gneiss; Lamp—lamprophyre; HblGn—hornblende gneiss.

Sample	z (m)	Lithology	λ_{PAR} ($Wm^{-1}K^{-1}$)			λ_{PER} ($Wm^{-1}K^{-1}$)		
			DB	OS	LS	DB	OS	LS
62H4s	423.4	Am	2.38	2.39	2.72	2.15	2.30	2.66
117G4ab	617.2	Gn	3.66	3.87	3.71	3.59	2.84	2.95
168B1j	800.9	Gn	4.14	3.71	3.59	3.34	2.76	3.13
207C4g	887.4	Gn	3.88	3.50	3.61	2.82	2.75	2.94
234D1aa	943.7	Gn	3.27	3.84	4.04	2.79	2.84	1.94
253D1k	1179.2	Am	2.38	2.58	2.55	2.31	2.44	2.35
284H1r	1361.1	Am	2.32	2.52	2.55	2.13	2.26	2.30
323B1d	1542.2	Am	2.32	2.10	2.66	2.16	2.07	2.29
349B1j	1661.3	Gn	3.92	3.63	3.41	3.27	2.79	3.19
402F6e	1788.6	Gn	3.64	3.46	–	..	3.32	–
443E2n	1961.9	Gn	3.82	3.82	4.32	2.15	2.35	2.10
471F1t	2063.4	Gn	3.12	3.58	3.61	2.23	2.29	2.05
480D1k	2098.8	Gn	3.55	3.69	–	2.14	2.10	..
505B2b	2181.3	Gn	3.57	3.77	3.26	2.56	2.52	2.37
532E1r	2244.2	Lamp	3.15	2.94	..	3.15	2.73	..
561D1t	2329.6	Gn	3.32	3.39	3.22	2.17	2.19	1.86
584A1b	2404.8	Gn	3.48	3.63	3.42	2.36	2.30	1.89
592A1f	2434.0	Gn	3.28	3.76	3.38	2.65	2.65	2.45
617B1cK	2532.9	HblGn	2.92	3.06	2.83	2.67	2.62	2.71
627B1h	2587.5	Gn	3.58	3.90	..	2.64	2.79	–
640A2a	2692.6	Gn	3.60	3.65	–	..	2.72	..
664F1sK	2768.6	Lamp	3.65	3.59	4.07	3.09	2.97	3.13
705D1l	2874.9	Gn	..	3.85	–	2.34	2.40	..
736B1f	3005.2	Gn	3.37	3.43	3.62	3.13	2.95	3.58
743C1f	3038.5	Gn	3.54	3.61	3.49	2.99	2.89	2.61
755B2g	3085.2	Gn	3.28	3.73	..	1.30	1.78	..
783E6av	3207.1	Gn	3.28	3.19	2.87	3.16	3.00	2.81
796A8eK	3262.5	Gn	3.38	3.26	..	–	2.28	..
804D1m	3299.6	Gn	3.66	3.47	2.96	2.44	2.31	2.88
815B1rK	3349.9	Gn	3.85	3.85	4.23	3.11	2.67	3.25
824E1n	3380.1	Gn	3.77	3.69	4.26	3.07	3.25	3.35
831A3b	3407.2	Gn	3.73	3.89	4.30	..	3.24	2.90
837D1k	3425.9	Gn	3.93	3.31	3.26	–	2.87	3.14
848E1p	3474.3	Gn	3.88	3.47	3.72	3.35	3.09	3.56
863E2af	3531.5	Gn	4.18	3.67	..	3.02	2.88	..
870C9g	3551.7	Gn	3.50	3.60	3.56	2.88	2.65	2.99
882A4j	3601.5	HblGn	2.64	2.46	2.53	2.55	2.17	2.49
891E1u	3647.8	Am	2.93	2.98	3.00	2.80	2.72	2.67
904E1h	3679.5	Am	2.44	2.56	–	2.30	2.16	–
909B1d	3706.4	Am	2.65	2.76	2.71	2.55	2.22	2.63
917B1cK	3748.1	Am	2.43	2.23	2.51	2.40	2.09	2.31
920C2d	3766.3	Am	2.54	2.45	2.40	2.38	2.31	2.38
938A1a	3829.7	Am	2.61	2.59	2.53	2.49	2.59	2.18
944E6s	3857.8	Am	2.60	2.50	2.27	2.36	2.31	2.21

Table 2
Results of thermal conductivity (λ) measurements from divided-bar (DB) and optical scanning (OS) methods parallel (λ_{PAR}) and perpendicular (λ_{PER}) to the foliation for Collection II (see text). z—depth; 3D anisotropy occurs when $\lambda_{PAR,1} \neq \lambda_{PAR,2}$ for OS; λ_V—transformation of OS results (eq. (5) for 3D anisotropy; eq. (7) for 2D anisotropy) corresponding to values from DB ($\lambda' \approx \lambda_{PAR}$; $\lambda'' \approx \lambda_{PER}$; for isotropic rocks: $\lambda' = \lambda''$). Lithology: AM—amphibolite; GN—gneiss.

z (m)	Lithology	OS			DB		
		λ_{PER}	$\lambda_{PAR,1}$	$\lambda_{PAR,2}$	λ_V	λ''	λ'
800.0	Gn	2.93	3.39	3.39	2.94	2.90	–
800.0	Gn	2.59	3.46	3.46	2.60	2.82	–
800.0	Gn	2.59	4.45	3.56	4.38	–	4.11
800.0	Gn	2.61	4.63	3.65	4.52	–	4.21
885.1	Gn	2.47	4.38	3.58	4.34	–	4.30
885.1	Gn	2.52	4.59	3.82	4.54	–	4.63
887.2	Gn	1.98	3.43	3.18	2.02	2.19	–
887.2	Gn	2.62	3.62	3.62	2.64	2.70	–
1273.5	Am	2.74	2.74	2.74	2.74	2.84	2.84
1273.5	Am	2.69	2.69	2.69	2.69	2.68	2.68
1357.6	Am	2.41	2.65	2.65	2.65	2.65	2.65
1357.6	Am	2.36	2.79	2.79	2.79	2.70	2.70
1746.3	Gn	2.78	4.36	3.67	4.34	–	4.30
1746.3	Gn	3.64	4.45	4.45	4.45	–	4.38
1746.3	Gn	2.78	4.07	3.67	4.05	–	4.19
1746.3	Gn	2.75	4.25	3.56	4.20	–	4.00
1746.3	Gn	2.60	3.88	3.88	2.60	3.20	–
1746.3	Gn	2.35	3.57	3.57	2.35	2.80	–
1859.7	Gn	2.56	3.64	3.22	2.57	2.39	–
1859.7	Gn	2.21	3.80	3.30	2.25	2.35	–
1859.7	Gn	2.13	4.00	3.46	3.97	–	–
1859.7	Gn	2.08	4.49	3.31	4.38	–	–
2447.3	Gn	2.88	4.35	3.99	4.33	–	4.61
2447.3	Gn	2.74	4.45	3.75	4.43	–	–
2447.4	Gn	2.91	3.79	3.79	2.91	2.94	–
2447.4	Gn	2.96	3.89	3.89	2.96	3.08	–
2497.0	Gn	2.26	3.30	2.97	3.30	–	3.18
2497.0	Gn	2.44	3.52	3.08	3.52	–	3.33
2497.1	Gn	2.58	2.97	2.97	2.58	2.66	–
2497.1	Gn	2.58	2.88	2.88	2.59	2.50	–
3146.1	Gn	2.63	3.68	3.68	3.45	–	3.62
3146.1	Gn	2.68	3.80	3.80	2.71	2.81	–
3146.2	Gn	2.68	3.72	3.72	2.68	2.96	–
3146.2	Gn	3.01	3.75	3.75	3.01	3.40	–
3723.7	Am	2.51	2.51	2.51	2.51	2.53	2.53
3723.7	Am	2.53	2.53	2.53	2.53	2.58	2.58

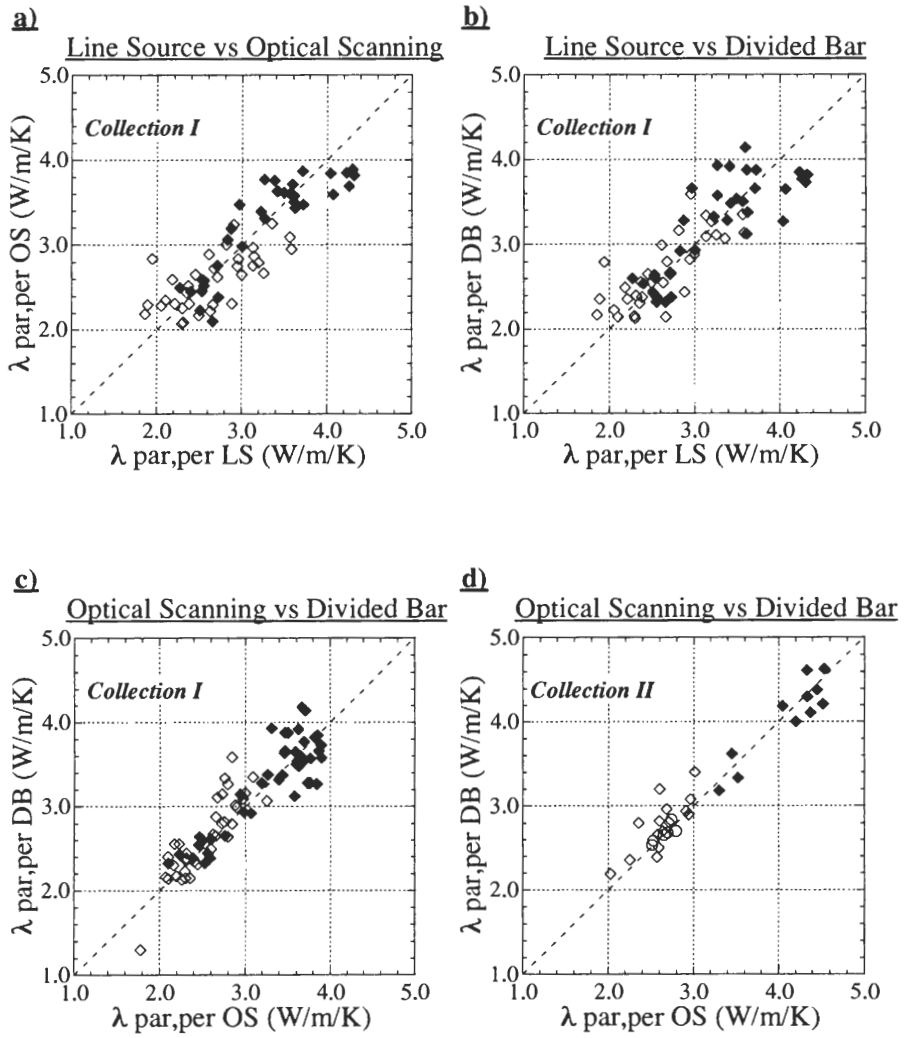

Fig. 8. Comparison of results. (a)–(c) Collection I; (d) Collection II; solid diamonds: thermal conductivity perpendicular to the foliation (λ_{PER}); open diamonds: thermal conductivity parallel to the foliation (λ_{PAR}); open circles: isotropic samples.

factor) is significant. This was also noted for Collection II, and possible sources of the discrepancy will be discussed below. The same tendency was noted for DB and LS results (see also Pribnow and Sass, 1995) but the significance of this difference is obscured by a more substantial random error of the LS.

Because many samples from Collection I are significantly inhomogeneous ($\varepsilon \approx 0.46$) and (in contrast to Collection II) the measured samples were not identical, the random

discrepancies in measurement results obtained with different methods may in many cases be explained by inhomogeneity.

4.2. The random error of LS

The comparison of methods indicates a lack of systematic differences in principal thermal conductivity values and anisotropy factors. The results obtained with LS are, however, more unstable than for other techniques. There are two apparently equally significant sources of this instability. The first is the relatively high random error of measurements with LS. From our study on six standard samples with a thermal conductivity range of 1.35–6.89 $Wm^{-1}K^{-1}$, and on 25 samples from the Kola borehole with thermal conductivity of 2.3–5.0 $Wm^{-1}K^{-1}$, the LS unit has a random error of single measurement in the range of 7–9% at 0.95 confidence level. In the course of n repeated measurements, the random error is reduced by a factor of $\sqrt{n}$, so that the random error of five measurements was 3–4%, still higher than for other methods. The second source of LS instability may be related to a local position of the temperature sensor in the probe. Comparison of LS and OS data for 25 inhomogeneous core samples from the Kola borehole indicates that readings substantially depend on the local thermal conductivity close to the sensor. This occurs despite a significant but incomplete equalization of temperature along the probe by its thin steel shell. For example, if the sensor was located above a grain with a thermal conductivity that exceeds the mean conductivity of the sample (derived from the OS measurement) by 50–60%, the readings of the LS were overestimated by 30–40% relative to the average value. When a zone of reduced conductivity occurred under the probe the readings were underestimated. For example, when the sensor was located above a short narrow crack the readings were 20% lower than the mean value. This can lead to a random measurement error of up to 10–15% for inhomogeneous samples. Because the factors causing LS instability are not correlated, the net random error of LS for measurements on samples from Collection I can reach 11–15% for this study. Recently, the interpretation of LS measurements has been significantly improved (H. Honarmand, pers. comm.), and in combination with greater experimental efforts the error of modern LS measurements can be reduced to 2%.

4.3. Collection II

For this collection, it was not always possible to prepare samples strictly perpendicular or parallel to the foliation. The angle between the foliation and the sample axis deviated up to 10° from the desired value (0° or 90°), and for one disk the angle was 60°. To correspond to a value obtained with DB, the OS measurements of λ_{PAR} and λ_{PER} were transformed into an effective thermal conductivity (λ_V) with eq. (5) or eq. (7). The DB results and the effective conductivity values obtained with OS can be considered in two groups: λ' close to λ_{PAR} ($90° \pm 10°$) and λ'' close to λ_{PER} ($0° \pm 10°$). Three-dimensional anisotropy (λ_A perpendicular to the foliation plane, λ_B and λ_C parallel to the foliation plane) was recognized for some samples with the OS technique (see also Table 2). Here, the λ_{PAR} range implies a combined range of both λ_B and λ_C.

Six massive amphibolite samples were devoid of preferred foliation orientation; OS results from these disks along three mutually perpendicular directions were not significantly different.

The correlation between λ_V (OS) and λ' or λ'' (DB) is shown in Fig. 8(d). If no anisotropy was detected with the OS, DB results were included in both data sets ($\lambda' = \lambda''$) in Table 2. As can be seen from Fig. 8, the consistency of DB and OS results for Collection II is better than for Collection I. This is due to the use of identical samples for measurements conducted with both methods and our taking into account the real inclination angles between the foliation and disc planes.

In general, for Collection II the discrepancy does not exceed $\pm 10\%$. Only three samples stand out because of somewhat higher differences. The thermal inhomogeneity factor for one of these samples was extremely high (0.33). The results of λ_{PER} (OS) and λ' (DB) for two samples from 1746 m depth deviate significantly more than all others (see Table 2). Possible reasons are not known yet but under investigation. However, as this deviation is statistically anomalous for this comparison, these results are excluded in the following analysis.

Similar to Collection I, linear regressions demonstrate consistency of OS and DB results: high values of correlation coefficients (0.78 to 0.98), linear coefficients close to 1 (0.91 to 1.1), and small intercepts (0.11 to 0.34) and standard deviations (0.16 to 0.20). The average relative difference for the λ' and λ'' data obtained with both methods is 2.1% and the standard deviation is 6.5%. The average relative difference is 0.7% (standard deviation is 3.9%) for λ', and 2.9% (standard deviation is 4.8%) for λ'' (4.6% with standard deviation of 6.8% if the two anomalous samples mentioned above are included in the analysis).

4.4. Aspects of high-resolution OS results

The effect of cracks that form an effective barrier for heat flow when dry but have a negligible effect when the rock is saturated is discussed by Walsh and Decker (1966) for stress relief dilatancy and by Pribnow et al. (1996) for thermally-induced cracks. In our experience studying cores derived from great depths, microcracks close to their cylindrical surface are often observed, reducing the thermal conductivity of the respective areas measured with OS on dry samples. In cores of exploration boreholes 500–700 m in depth, we have not commonly observed a noticeable change. However, thermal conductivity reductions in the outer layer (7–12 mm thick) of drill cores were observed for deeper drill holes: 7–8% for crystalline rocks from the Kola borehole (2–10 km depth, Lat.: 69 00 25 N, Long.: 30 00 44 E, the Kola Peninsula), 14–20% for crystalline rocks recovered from the Ural borehole (depth to 5.3 km, Lat.: 58 00 00 N, Long.: 59 00 44 E, the Ural Mountains), and 20–30% for sedimentary rocks from the Timan–Pechora borehole (7 km deep, Lat.: 65 00 32 N, Long.: 46 00 12 E, northern part of the European territory of Russia). By analogy, a similar drop in thermal conductivity could be expected for the outer layers of disks from KTB rocks. However, the introduction of appropriate corrections led to an insignificant but noticeable deviation from the DB and LS results, which are based on water-saturated samples and thus are only minimally influenced by the effect of microcracks. Further, samples

of massive amphibolites show virtually complete coincidence of conductivity measurements on plane and cylindrical surfaces of disks without any correction. The introduction of stress-relief corrections for cylindrical surfaces of disks was thus rejected.

For two disks (gneiss samples from a depth of 2497.05 and 3146.21 m), the OS resulted in significant differences (18 and 12%, respectively) for opposite planes only 8–12 mm apart. This indicates a substantial sample inhomogeneity along the disk axes. A detailed examination of these samples has shown that, in the first case, the heterogeneity is related to the occurrence of dark-colored minerals on one face whereas light-colored minerals of higher thermal conductivity are predominant on the opposite face. In the second case, the inhomogeneity was caused by an enrichment of quartz on one face, and this face has a higher thermal conductivity. In order to study the inhomogeneity of these samples and to estimate their conductivity more precisely, measurements on both planes of each disk were carried out with the distance between the heated spot and the temperature recorder increased by a factor of 6; this allowed us to increase the thickness of the measured surface-layer approximately 2.5 times and to actually accomplish thermal sounding throughout the sample. The results establish that thermal conductivity varies with depth in an irregular manner, and this variation was taken into account in the computation of the principal values.

Repeated thermal conductivity measurements were performed for three disks after their saturation in water for 6–7 h. These disks represent gneisses with high anisotropy factors: 1.46, 2.16. and 1.51 for samples from 1746.30 m, 1859.73 m and 2447.28 m, respectively. After saturation, there was no significant change in conductivity components along the foliation, whereas the component oriented perpendicular to the foliation increased by 3.8, 4.8, and 1.5%, respectively, relative to the values for the dry samples. Taking into account the random error of single measurements (1.6% at 0.95 confidence interval), this variation is considered to be significant. This indicates some contribution of oriented fracturing to the anisotropy, which is mainly caused by micas occurring in the gneiss. These fractures will have little effect in a parallel configuration (along bedding), but when they are in series with the minerals saturation should increase thermal conductivity, as we observed. These observed effects of saturation on λ_{PER} are consistent with the average relative difference between λ'' (saturated DB) and λ_{PER} (unsaturated OS).

A 3-D anisotropy was established for 16 of the 36 samples measured with the OS. The most favorable conditions for the study of anisotropy existed when the foliation was parallel or nearly parallel to the disk plane. In this case, the foliation and a clear lineation in grain arrangement were helpful in the precise choice of principal conductivity axes. The first axis was perpendicular to the foliation and the second and the third axes lay in the foliation plane parallel and perpendicular to lineation. More complicated problems related to the principal axis choice arose when the foliation was oriented perpendicular or nearly perpendicular to disk planes. In cases of proven 3-D anisotropy, the anisotropy ratio lies within the range of 1.42–2.16; the mean value is 1.66, and the standard deviation is 0.19. The two principal values corresponding to the foliation plane are closer to equal than the value perpendicular to the foliation plane. For the case of 2-D anisotropy, the range of anisotropy factor is 1.10–1.52, the mean value is 1.30, and the standard deviation is 0.14.

5. Summary

Because we chose frequently-used instruments with a prolific data output that typify the methods compared, the results obtained are of general significance. The DB unit used in this study was constructed by the U.S. Geological Survey in the late 1960s (Sass et al., 1971b) and continually studied and improved (Pribnow and Sass, 1995). The LS unit was created on the basis of previously proposed scientific recommendations and applied to numerous measurements of thermal conductivity on cores of KTB boreholes (Huenges et al., 1990). OS apparatuses were conceived (Popov et al., 1985a), studied, and developed in the 1980s and 1990s in the course of their application to conductivity measurements on more than 70,000 samples from various geological objects, including over 23,000 core samples from Russian scientific deep boreholes. The careful comparisons among the three independently developed methods provide strong empirical validation of all of them.

In general, the deviation of the results from the three methods is less than 4%. For samples with a thermal inhomogeneity factor of less than 0.1, the agreement of the results is better than 2%. The DB and OS show the best agreement; a higher scatter of the LS is the consequence of point temperature measurements. For all three methods, values parallel to the foliation agree better than the perpendicular components. This is expected to be the case if the anisotropy is not 2-D (as assumed) but 3-D. In average, the DB reveals the lowest anisotropy factors, as a result of the difficulty of preparing samples accurately oriented parallel and perpendicular to the foliation. Comparing identical (Collection II) rather than closely-spaced (Collection I) samples improved the agreement between OS and DB. The high-resolution measurements with the OS revealed additional aspects of thermal conduction, such as small-scale inhomogeneities of mineral composition and artificially introduced micro-cracks.

Although we cannot propose an unequivocal explanation for a small but statistically significant difference in λ_{PER} measurements for both collections, some possible causes may be suggested: (1) water saturation of the DB and LS samples that minimizes the effects of fracturing parallel to the foliation; (2) closure of cracks aligned with the foliation under the axial load of the DB; (3) fracturing along foliation and bedding due to residual internal stresses that arose in deep-derived samples during two years between DB and OS measurements (as observed in cores from Vorotilovo and Tyumen boreholes); and (4) regularities in heat transfer previously established for isotropic materials studied with DB and LS may be disturbed in the case of anisotropic rocks. Anisotropy might require some corrections to recommended relationships between the sample size and the device elements. In particular, it is possible to quantify enhanced radial heat losses in DB study of disks with the axes perpendicular to the λ_{PAR} direction.

6. Conclusions

Numerous measurements of thermal conductivity on isotropic and anisotropic rocks carried out with divided-bar, line-source, and optical scanning indicate that

these methods yield consistent results. Significant inhomogeneity of rocks is a possible reason for the observed minor discrepancies. The closest agreement was noted between DB and OS. Widespread use of the contactless OS method should provide a dramatic increase in the information output from the study of rock conductivity. This high-speed method provides (1) measurement of principal values of thermal conductivity both for 2-D and 3-D anisotropic samples; (2) recording of thermal conductivity distribution at each sample with determination of local values; and (3) measurement on both plane and cylindrical surfaces without any severe constraints for sample size and quality of surface treatment. The application of OS allowed us to obtain new information on thermal inhomogeneity and the three-dimensional anisotropy of rocks from the KTB borehole.

We have shown conclusively that the three methods are interchangeable, within their combined errors, for the characterization of thermal conductivity. Details of the specific application and the degree and kind of technical assistance available will have a strong bearing on which method is chosen in a given instance. For example, the DB will be the technique of choice when an unambiguous characterization of thermal conductivity in a given direction is the goal and when the appropriate rock-machining equipment and skilled personnel are available. The LS provides a convenient configuration for reconnaissance surveys of large numbers of thermally nearly isotropic rocks. It is also the most easily adapted to measurements at elevated temperatures, particularly for saturated rocks (e.g. Williams and Sass, 1996). OS methods are also well suited to reconnaissance surveys, especially when sample size is an issue. They are useful in examining the details of heat conduction in samples with complex structure and composition.

Acknowledgements

Constructive criticism and valuable suggestions by Will Gosnold, Dave Blackwell, Steve Ingebritsen and Paul Morgan helped to improve this manuscript. Sue Priest and Juliane Herrmann improved many of the figures. The authors would like to thank Christoph Clauser and Hans Burkhardt for finding funds from the German science foundation DFG and the European Union's INTAS program to finance Yuri Popov's visits in Germany. The authors would also like to thank Hubert Köstler and Robert Fürnrohr for preparing most of the rock samples, and Armin Rauen and Thomas Röckel for helping with the sample collection.

References

Beck, A.E., 1987. Methods for determining thermal conductivity and thermal diffusivity. In: Haenel, Rybach, Stegena, (Eds.), Handbook on Terrestrial Heat Flow Density Determination. Kluwer, Dordrecht, pp. 87–124.

Birch, F., 1950. Flow of heat in the Front Range. Colorado. Geological Society of America Bull. 61. 567–630.

Blackwell, D.D., Spafford, R.E., 1987. Experimental methods in continental heat flow. In: Sammisaud, Henyey, (Eds.), Methods of Exp. Phys., vol. 24. Academic Press, New York, chapter 14, pp. 189–226.

Bullard, E.C., 1939. Heat flow in South Africa. Proceedings of the Royal Society of London A 173, 474–502.

Burkhardt, H., Honarmand, H., Pribnow, D., 1990. First results of thermal conductivity measurements with a borehole tool for great depths. In: Bram, Draxler, Kessels, Zoth, (Eds.), KTB Report, vol. 90–6a. Springer Verlag, Hannover, pp. 245–258.

Carslaw, H., Jaeger, J.C., 1947. Conduction of Heat in Solids. Clarendon Press, Oxford.

Grubbe, K., Haenel, R., Zoth, G., 1983. Determination of the vertical component of thermal conductivity by line source methods. Zeitblatt für Geologie und Palaontologie, Teil I H (1/2), 49–56.

von Herzen, R.P., Maxwell, A.E., 1959. The measurement of thermal conductivity of deep-sea sediments by a needle probe method. Journal of Geophysical Research 64, 1557–1563.

Huenges, E., Burkhardt, H., Erbas, K., 1990. Thermal conductivity profile of the KTB pilot corehole. Scientific Drilling 1, 224–230.

Jaeger, J.C., 1958. The measurement of thermal conductivity and diffusivity with cylindrical probes. EOS Trans. AGU 39, 708–710.

Jaeger, J.C., 1959. The use of complete temperature–time curves for determination of thermal conductivity with particular reference to rocks. Australian Journal of Phys. 12, 203–217.

Lachenbruch, A.H., 1957. A probe for measurements of thermal conductivity of frozen soils in place. Eos Transactions AGU 38, 691–697.

Lewis, T., Villinger, H., Davis, E., 1993. Thermal conductivity measurement of rock fragments using a pulsed needle probe. Canadian Journal of Earth Sciences 30, 480–485.

Popov, Y.A., 1983. Theoretical models of the method of determination of the thermal properties of rocks on the basis of movable sources. Geologiya i Razvedka (Geology and Prospecting) Part I, 9, 97–103 (in Russian).

Popov, Y.A., 1984a. Theoretical models of the method of determination of the thermal properties of rocks on the basis of movable sources. Geologiya i Razvedka (Geology and Prospecting) Part II, 2, 83–86 (in Russian).

Popov, Y.A., 1984b. Peculiarities of the method of detailed investigations of rock thermal properties. Geologiya i Razvedka (Geology and Prospecting) 4, 76–84 (in Russian).

Popov, Y.A., Semionov, V.G., Korosteliov, V.M., Berezin, V.V., 1983. Non-contact evaluation of thermal conductivity of rocks with the aid of a mobile heat source. Izvestiya, Physics of the Solid Earth 19, 563–567

Popov, Y.A., Berezin, V.V., Semionov, V.G., Korosteliov, V.M., 1985a. Complex detailed investigations of the thermal properties of rocks on the basis of a moving point source. Izvestiya, Physics of the Solid Earth 1, 64–70.

Popov, Y.A., Berezin, V.V., Semionov, V.G., 1985b. Evaluating the thermal conductivity of anisotropic minerals and rocks. Izvestiya, Physics of the Solid Earth 7, 565–570.

Popov, Y.A., Berezin, V.V., Soloviov, G.A., Romuschkevitch, R.A., Korosteliov, V.M., Kostiurin, A.A., Kulikov, A.V., 1987. Thermal conductivity of minerals. Izvestiya, Physics of the Solid Earth 3, 245–253.

Popov, Y.A., Korosteliov, V.M., Berezin, V.V., Romuschkevitch, R.A., 1991. Thermal physical investigations of rocks and ores. Sovetskaya Geologiya (Soviet Geology) 6, 43–48 (in Russian).

Popov, Y.A., Mandel, A.M., 1998. Geothermic investigations of anisotropic strata. Izvestiya, Physics of the Solid Earth 11, 33–43.

Popov, Y.A., Mandel, A.M., Kostyurin, A.A., Bangura, A., 1990. New methodological opportunities for investigations of thermal conductivity of anisotropic rocks and minerals. Geologiya i Razvedka (Geology and Prospecting) 8, 85–90 (in Russian).

Popov, Y.A., Rabe, F., Bangura, A., 1993. Adequacy of theoretical and experimental models of the optical scanning method. Geologiya i Razvedka (Geology and Prospecting) 6, 65–72 (in Russian).

Pribnow, D., Sass, J.H., 1995. Determination of thermal conductivity from deep boreholes. Journal of Geophysical Research 100, 9981–9994.

Pribnow, D., Williams, C., Burkhardt, H., 1993. Log-derived estimate for thermal conductivity of crystalline rocks from the 4 km KTB Vorbohrung. Geophysical Research Letters 20, 1155–1158.

Pribnow, D., Williams, C., Sass, J.H., Keating, R., 1996. Thermal conductivity of water-saturated rocks from the KTB pilot hole at temperatures of 25 to 300°C. Geophysical Research Letters 23, 391–394.

Sass, J.H., Lachenbruch, A.H., Munroe, R., 1971a. Thermal conductivity of rocks from measurements on fragments and its application to heat flow determinations. Journal of Geophysical Research 76, 2291–3401.

Sass, J.H., Lachenbruch, A.H., Munroe, R.J., Green, G.W., Moses Jr., T.H., 1971b. Heat flow in the western United States. Journal of Geophysical Research 76, 6376–6413.

Schön, J.H., 1996. Physical Properties of Rocks: Fundamentals and Principles of Petrophysics. Trowbridge.

de Vries, D.A., Peck, A.J., 1958. On the cylindrical probe method of measuring thermal conductivity with special reference to soils. Australian Journal of Phys. 11, 255–271.

Walsh, J., Decker, E., 1966. Effect of pressure and saturating fluid on the thermal conductivity of compact rock. Journal of Geophysical Research 71, 3053–3061.

Wilhelm, H., 1990. A new approach to the borehole temperature relaxation method. Geophysical Journal International 103, 469–481.

Williams, C.F., Anderson, R.N., 1990. Thermophysical properties of the Earth's crust: *in situ* measurements from continental and ocean drilling. Journal of Geophysical Research 95, 9209–9236.

Williams, C.F., Sass, J.H., 1996. The thermal conductivity of rock under hydrothermal conditions: measurements and applications. Proc. 21st Workshop on Geothrm. Res. Engr., Stanford University, pp. 335–341.